Article:

Mendez, J.E. orcid.org/0000-0001-5552-9030, McLaggan, M.S. orcid.org/0000-0002-4173-5615 and Lange, D. orcid.org/0000-0002-4551-1045 (2025) Upward flame spread behaviour of cladding materials on a medium-scale ventilated façade. Construction and Building Materials, 478. 141047. ISSN 0950-0618

https://doi.org/10.1016/j.conbuildmat.2025.141047

Construction and Building Materials 478 (2025) 141047

Contents lists available at ScienceDirect

Construction and Building Materials

journal homepage: www.elsevier.com/locate/conbuildmat

Upward flame spread behaviour of cladding materials on a medium-scale ventilated façade

Julian E. Mendez [a,*], Martyn S. McLaggan [b], David Lange [a]

[a] School of Civil Engineering, The University of Queensland, 4072, Queensland, Australia
[b] School of Mechanical, Aerospace and Civil Engineering, University of Sheffield, Sheffield, S1 3JD, UK

ARTICLE INFO

Keywords:
Cladding
Façade fire
Flame spread
Fire growth
Ignition
Heat release rate

ABSTRACT

A parametric experimental study was performed to characterise the phenomena governing the upward flame spread dynamics in a simplified ventilated façade using a medium-scale testing rig. The ventilated façade was comprised of an insulation foam (INS) and an aluminium composite panel (ACP) with a cavity between the two materials. Two different cavity widths (0.10 and 0.15 m), two INS products (Polyisocyanurate (PIR) and Phenolic (PF) foams) and two ACP cores (Polyethylene (PE) and Polyethylene based with fire retardant (FR)) were tested, for a total of 8 configurations. The experimental medium-scale set-up provides a fundamental understanding of the interactions between insulation materials and ACPs in fire growth in ventilated façade systems. High instrument density allows the use of bench scale flammability data to interpret the materials' contribution to the total HRR and analyse overall results. The study suggests the possibility of developing a comprehensive framework to assess fire performance of different material combinations and system layouts, improving fire safety standards in construction. Loss of encapsulation integrity was found to accelerate fire growth and flame spread on combustible linings. PIR and PF insulation materials contribute earlier to HRR and fire growth compared to ACP cores, with PIR contributing more. The smaller cavity width was observed to enhance the flame spread over the linings, with sustained spread in all cases whereas in the larger cavity width there were cases with unsustained spread. A fire growth parameter (γ) was quantified, with $\gamma < 0.005$ indicating unsustained spread over the linings, and values between 0.005 and 0.018 signifying sustained spread. The Cladding Materials Library framework enables reliable interpretation of observed behaviour and interactions between the materials studied and a fire within the cavity.

1. Introduction

In response to incidents like the Grenfell Tower fire, extensive research has focused on understanding and predicting the rate of upwards flame spread on cladding materials and systems. Various models have been proposed to estimate flame spread velocity; however, many of these models oversimplify the complex interactions within the system [1]. Additionally, parallel wall configurations have been employed to experimentally assess upward flame spread in different polymeric and cellulosic materials within a cavity. However, the underlying physical mechanisms behind this phenomenon have not been thoroughly explored. Existing studies have primarily examined the impact of the cavity on either the HRR or the flame spread rate, without considering both simultaneously. Additionally, the relationship between a narrow cavity width and any enhancement of thermal feedback between the components remains unexplored. Further investigation in this area is crucial to obtain a comprehensive understanding of fire behaviour to better contribute to the fire safe design of high-rise buildings. A review of relevant models for the characterisation of upward flame spread in ventilated façades is presented in Sections 1.1 to 1.4, further review can be found in the literature [2,3].

1.1. Flame spread fundamentals

Flame spread occurs when heat transfers from a burning region to an adjacent unburnt fuel, leading to subsequent ignition and fire propagation. This process involves three primary heat transfer modes: convection in the gas phase, radiation from the flame or external sources, and conduction in the solid fuel. The heat flux to the unburnt area ($\dot{q}''$) causes ignition and flame spread, occurring primarily in the pyrolysis zone where the fuel decomposes [4]. The flame spread rate (V_p) can be expressed through an energy balance equation, as shown in Eq. (1). Alternatively flame spread can be characterised in terms of

* Corresponding author.
E-mail address: j.mendez@uq.edu.au (J.E. Mendez).

https://doi.org/10.1016/j.conbuildmat.2025.141047
Received 22 December 2024; Received in revised form 27 February 2025; Accepted 24 March 2025
Available online 24 April 2025

the heat flux received by the unburnt region and fuel properties such as density, thermal conductivity, and specific heat capacity [5,6], as well as external conditions like the initial fuel temperature [7] and external heat flux [8,9]. Eqs. (1) and (2) derived from these principles govern the relationship between flame spread rate, heat flux, and material properties. Additional flame spread models are discussed in the following section.

$$V_p \rho \Delta h = \dot{q}'' \tag{1}$$

$$V_p = \frac{\dot{q}''}{\rho c_p (T_{ig} - T_0)} \tag{2}$$

1.2. Upward flame spread mechanisms and models

Upward flame spread presents a unique challenge because of the natural buoyancy of flames, which promotes a concurrent spread along vertical surfaces. This process is complex due to the non-steady heat transfer and varying physical and chemical properties of the fuel. A simplified representation of flame spread, incorporating the burnout, pyrolysis, and preheated lengths, has been used in many studies [10–12]. One key model for upward flame spread, proposed by Orloff et al. [10] in Eq. (3), is based on the pyrolysis length (x_p), flame length (x_f), and forward heat flux. Orloff [10] developed a theory predicting flame spread velocity for thermally thick materials like polymethyl methacrylate (PMMA), showing that flame spread increases asymptotically to a steady value. Further developments by Markstein and deRis [13] investigated flame spread over textiles, demonstrating that flame velocity increases with time but eventually reaches a constant rate. Markstein and deRis presented a simplified empirical model (see in Eq. (4)), that considers a relatively constant fire growth rate factor $\gamma = V_p/x_p$, and represents an exponentially increasing fire size.

$$V_p = \frac{x_p}{\tau}\left(\frac{\ln n}{(n-1)}\right)\ln\left(x_f/x_p\right) \tag{3}$$

$$x_p = x_p\Big|_{t=0}\gamma \qquad exp(\gamma\ t) \tag{4}$$

Other models, such as those proposed by Sibulkin and Kim [14], relate flame spread velocity to surface heat flux and preheated length (δ_{ph}). Quintiere et al. [15] introduced a multiplication factor for the preheated length in Eq. (5), refining the prediction of flame spread velocity for various materials.

$$V_s = \frac{4}{\pi}\frac{\left(\dot{q_f}''\right)^2\delta_{ph}}{\rho_s c_{p_s} k_s \left(T_p - T_\infty\right)^2} = \frac{\delta_{ph}}{\tau_{ig}} \tag{5}$$

where τ_{ig} is the characteristic time for ignition, which only depends on material properties. The model in (5) assumes a constant value for the flame heat flux over the preheated length. This is valid for single burning items and values ranging from 15-35 (kW m^{-2}) which have been used in the literature [16]. Much larger values for the flame heat fluxes can be observed as the burning rate increases which occur in larger fires [17] for upward flame spread in corner and or parallel wall setups [18–22]. An increase of the external heat flux has been observed when reducing the cavity width in a number of studies [18–20]. However, an existing gap is that no model has been obtained for the effect of the cavity width on the flame spread velocity over combustible linings in a parallel wall arrangement. Despite the fact that the effect of geometry on the incident heat flux on the walls has been described, this has not been coupled to the ignition and subsequent fire spread along the cladding materials.

1.3. Flame spread in parallel wall configurations

Parallel wall configurations significantly influence flame spread due to enhanced heat feedback between the two walls and restricted airflow, which accelerates flame propagation. Schlyter [23,24] first designed an experimental setup to test vertical fire spread between parallel panels. Later, this was adapted by the U.S. Forest Products Laboratory [25] to evaluate fire retardant coatings on wood-based materials.

The “Schlyter Effect”, coined by Babrauskas [26], refers to the phenomenon where materials that show limited burning in single-wall configurations exhibit increased fire severity when a second panel is introduced, creating a flue between the two. The small air gap promotes buoyancy-driven airflow, enhancing flame spread. LeVan [27] and Dietenberger [28] experimentally confirmed that this effect accelerates flame spread, especially in tests such as the Modified Schlyter Test.

More recent studies by Tsai [22] and Shih and Wu [29] explored flame spread in different geometric configurations, such as corners and U-shaped structures. Their research indicated that configurations with enclosed or narrowed gaps, such as parallel walls with reduced cavity width, promote faster flame spread due to enhanced thermal feedback and limited airflow.

1.4. Previous research on flame spread in ventilated façade systems and components

The behaviour of ventilated façade systems in fire scenarios has been the focus of extensive research. Choi and Taylor [30] conducted a study on the flame spread in ventilated façades featuring foamed plastic insulation, which revealed that ventilation in cavities significantly affects fire growth, with a critical cavity width of 25 mm identified for promoting rapid flame spread, as previously observed by Taylor [31].

Several researchers have investigated the effect of cavity width and cladding materials on flame spread in façade systems. For example, Tsai [22] and Shih [29] studied upward flame spread in parallel wall configurations and found that narrower cavity widths, such as 50 mm, lead to faster flame propagation compared to larger gaps or single-wall setups. Studies conducted at FM Global, such as the Parallel Panel Test (PPT), were developed as a cost-effective alternative to full-scale fire testing in corner setups [32,33]. These tests generate heat fluxes consistent with expected real-world conditions for cavity fires. Agarwal [21] used this method to assess the fire performance of cladding assemblies and found that polyethylene (PE) core aluminum composite panels (ACPs) exhibited rapid flame spread, while fire-retardant materials limited flame growth. Research at the University of Edinburgh concluded that heat transferred from the opposing wall to the ACP-PE is likely to drive the flame spread over the ACP and the relative contribution of this material to the total heat released, whereas the combustibility of the opposing wall was shown to be of secondary importance for the flame spread [34]. Sharma and Mishra developed an experimental parallel-wall setup incorporating different combustible ACPs and insulation foams (Expanded polystyrene, Polyisocyanurate and Mineral wool). The setup was intended for the initial screening of façade assemblies at lab-scale. The study emphasised that the high pressure differential and re-radiation between the walls led to higher mass burning rate, flame height and temperature in the cavity. The study provides measurements of flame height but the overall HRR was not measured and the contribution of individual materials to the total HRR was not discussed either. [35] Guillaume et al. [36] quantified the HRR for ACP-insulation systems as a whole, without quantifying the individual contribution of the components, and emphasis was made on the differences between systems with PE core versus ones containing PE and a fire retardant (FR). Garvey et al. [37] presented a method for quantifying the individual contributions of cladding materials to the total HRR, by using the thermal properties obtained during the material characterisation. The authors found that an ACP core with a higher organic content dominated the HRR of the systems where it was included, while the insulation type governed the fire growth in the systems using an ACP with a fire retardant and lower organic content.

The research undertaken by Garvey was done within the context of the development of the Cladding Materials Library database developed at the University of Queensland in collaboration with the Non-Conforming Building Products (NCBP) Audit Taskforce in the State of Queensland (Australia) [38]. The framework behind the database is intended to provide a robust methodology to assess the fire hazard of cladding materials in existing buildings based on a thorough understanding of the relevant fire phenomena [39].

A number of articles that study the fire behaviour of ventilated façades comprised by other types of materials such as glazing. However, since the assemblies are comprised of non-combustible components, it is fire performance will be governed by other types of interactions. Sun et al. [40] conducted an experimental campaign (based on the JIS A 1310 configuration), and numerical validation to assess the fire performance of double skin glazed façades. The study concluded that the cavity effect can enhance the fire load significantly, but that the cavity size has less effect on flame length than the overall HRR. The study also showed that the cavity size minimally influenced the HRR within the cavity, which contrasts with findings in systems with combustible materials. This difference can be attributed to the contribution of the combustible linings to the overall HRR and its faster burning rate with smaller cavity widths, as observed by Mendez et al. [41].

Research in the field of cladding materials and fire performance has been previously performed, but several gaps persist. These gaps include: linking available knowledge of materials and their characteristics with their behaviour during fire incidents, particularly their thermal properties; and more comprehensively investigating the influence of geometry on flame spread on cladding materials. Analysing the contribution of individual cladding system components to overall HRR is another area for further analysis. Addressing these gaps would strengthen the knowledge base and contribute to improved fire safety in building design and construction.

1.5. Aim and objectives

While previous studies have investigated how individual components' thermal properties affect the fire performance of the system, the effect of interactions between components and the role of the cavity in influencing fire growth remain unexplored. The primary objective of this paper is therefore to determine the conditions that enhance the flame spread in linings installed on a cavity, and understand how cavity width interacts with cladding materials to either promote or hinder fire growth. Through a comprehensive experimental campaign, the paper unravels the physical mechanisms and interactions governing flame spread in a ventilated façade with combustible cladding materials. By extracting the relative contributions of cladding products to fire growth and flame spread, this study aims to provide valuable insights that inform better design practices for enhanced fire safety.

2. Experimental approach

2.1. Simplified ventilated façade system

The experimental methodology relies on the use of a reduced scale experimental ventilated façade system, comprised of two 1,800 x 600 mm parallel walls with a variable width cavity. This setup represents a simplified section of a façade comprised of an exterior ACP, adjacent to a cavity and an insulation foam panel in the inner side of the system as depicted in Fig. 1(a). The façade assembly was placed on top of a sand gas burner with a length of 480 mm and a width matching the cavity width (see Fig. 1(a)). The ACPs and insulation panels used in the systems were mechanically fixed to a light-weight aluminium frame.

The ACP was fixed to the frame at the top, sides, and bottom of the panel by using eleven connection points (see Fig. 1(b)). The ACP was not directly fixed to the frame to reduce heat transfer to the frame, instead brackets were used to provide separation (Fig. 1(c)). These connection points were provided in order to reduce the thermal bowing effect previously observed on this type of materials when subjected to external heating. Two plasterboard panels were attached to the back of the insulation foam boards by using six threaded rods distributed across the height of the wall, to ensure that the encapsulation surfaces of the ACPs and insulation foam were kept parallel (Fig. 1(d)). The plasterboard sheets were installed to provide thermal protection to the structure and to provide stiffness to enable the installation of instrumentation through the rear face of the insulation panel. The setup allowed for the systematic replacement of the ACPs and insulation products. The cladding materials were mounted on an aluminium frame which allowed the cavity separation (W) to be varied.

The separation between the two parallel walls was set to either 100 or 150 mm. This cavity was left open laterally and on the top of the rig while a sand methane burner was located at the bottom of the cavity. The air entrainment was restricted at the bottom of the setup by the mounting frame and tailored non-combustible materials. The length of the burner was kept constant at 480 mm. This dimension was set to be shorter than the wall width (600 mm) to avoid the flames escaping the cavity before the ignition of the ACPs or insulation products. A burner with a width identical to the cavity width was installed for each test.

The fire source was placed within the cavity to generate the ignition of both the ACP and insulation material. The sand gas burner had a nominal flow rate of 30.5 $\mathrm{l\ min^{-1}}$ of methane (approximate effective heat of combustion 52,500 $\mathrm{kJ\ kg^{-1}}$), corresponding to a linear HRR of 35 kW m (nominal HRR of 16.8 kW). Three factors were taken into consideration when choosing the burner HRR:

1. that the HRR per unit length would be within the range of values previously studied in the literature;
2. that the HRR from the burner could be precisely quantified by oxygen consumption calorimetry, allowing for the identification of the contribution to the total HRR from the façade products; and
3. that the flame initially by the burner would not extend over the entire height of the experimental setup, so flame spread analysis could be performed.

The experimental rig was positioned under an extraction hood that allowed the exhaust gases to be sampled to determine the total HRR ($\dot{Q}$) through Oxygen Consumption calorimetry.

2.2. Products

Four different products were used in this parametric study corresponding to two ACPs and two foil-faced composite insulation foams (INS). A brief description of the products is presented below while a more detailed characterisation can be found elsewhere in the literature [3,41].

- Aluminium composite panel with high (90%) organic content core (PE): with a core thickness of 3 mm and 0.5 mm thick aluminium encapsulation.
- Aluminium composite panel with fire retardant (50%) and organic material (46%) core (FR): with a core thickness of 3 mm and 0.5 mm thick aluminium encapsulation.
- Polyurethane-based polyisocyanurate foam (PIR): with a thickness of 80 mm and aluminium foil (10 μm thick).
- Phenolic foam — organic foam insulation (PF): with a thickness of 80 mm and foil (10 μm thick, comprised of aluminium and a fibreglass grid).

The thermal properties of the cladding materials were determined using the Detailed Testing Protocol from the Cladding Material Library (CML) [42] and are presented in Table 1.

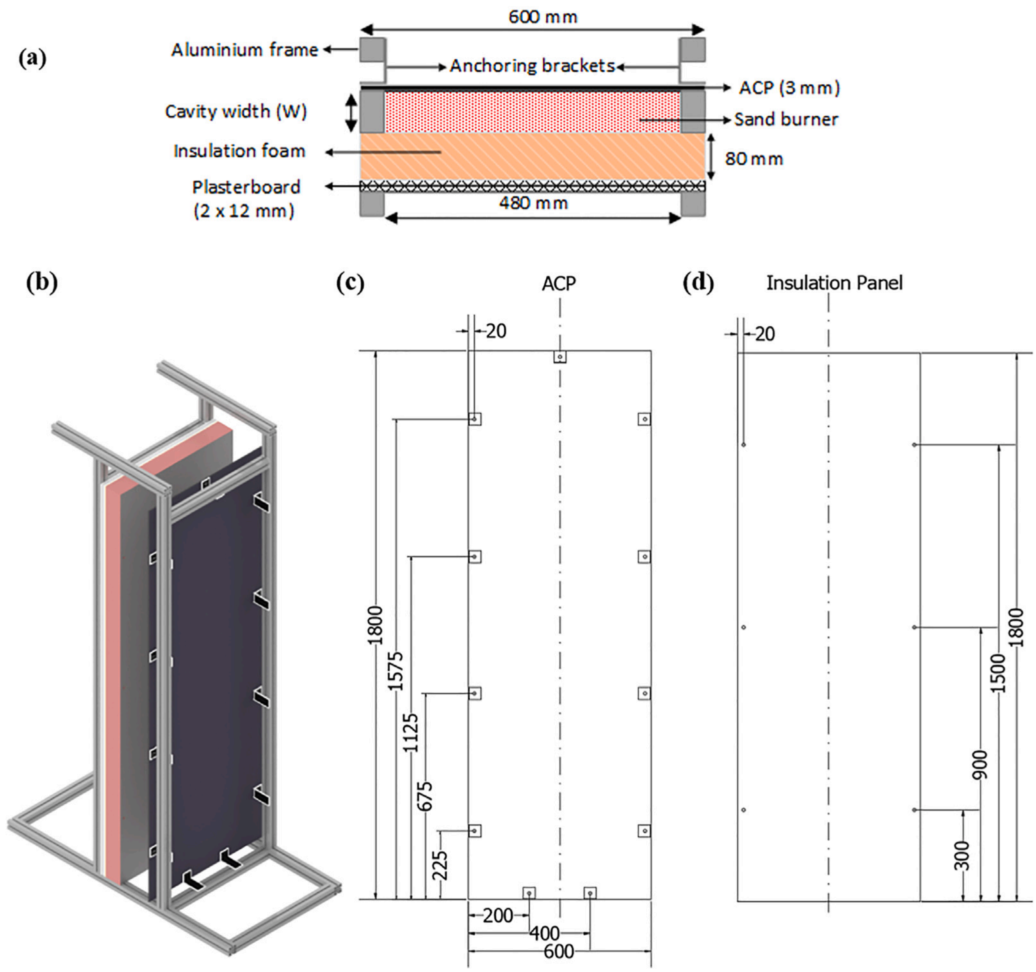

Fig. 1. Experimental setup components. (a) Top view. (b) Isometric view, the black elements represent the brackets. (c) Connection points for the ACP. (d) Connection points for the insulation foams.

Table 1
Cladding materials properties.

Material	ACP-FR	ACP-PE	PIR	PF
Description (CLM key name)	ACP with a core consisting of polyethylene and a fire retardant	ACP with a core consisting of polyethylene	Polyurethane-based polyisocyanurate foam (INS01)	Phenolic foam (INS02)
Gross heat of combustion ($\mathbf{kJ.g^{-1}}$)	20.14	38.98	30	26.5
Apparent thermal inertia ($\mathbf{kW^2.s.K^{-2}.m^{-4}}$)	1.122	1.273	0.037	0.08
Ignition temperature (**°C**)	423	321	458	417
Critical heat flux for ignition ($\mathbf{kW.m^{-2}}$)	19.5	11.5	23	18.9
Heat flux range ($\mathbf{kW.m^{-2}}$)	35–60	35–60	35–60	35–60
Peak heat release rate per unit area ($\mathbf{kW.m^{-2}}$)	131–175	397–615	150–223	62–89
Core thickness (**mm**)	3	3	80	80
Encapsulation thickness (**mm**)	0.5	0.5	0.01	0.01

Table 2
Experimental campaign conditions. Two repetitions (R1/R2) were carried for each configuration.

Test ID	Actual average gas burner HRR' ($kW.m^{-1}$)	Gas burner duration (min)	Cavity Width (mm)	ACP	Insulation board
FR.PIR.W150.R1	35.0	43	150	FR	Polyisocyanurate foam (PIR)
FR.PIR.W150.R2	35.0	40			
FR.PF.W150.R1	35.0	39			
FR.PF.W150.R2	35.0	40			
PE.PIR.W150.R1	35.2	8		PE	Phenolic foam (PF)
PE.PIR.W150.R2	35.0	8			
PE.PF.W150.R1	34.8	7			
PE.PF.W150.R2	35.0	5			
FR.PIR.W100.R1	35.0	38	100	FR	Polyisocyanurate foam (PIR)
FR.PIR.W100.R2	35.0	40			
FR.PF.W100.R1	35.0	28			
FR.PF.W100.R2	35.0	40			
PE.PIR.W100.R1	35.0	9		PE	Phenolic foam (PF)
PE.PIR.W100.R2	35.2	8			
PE.PF.W100.R1	35.2	9			
PE.PF.W100.R2	35.2	9			

2.3. Experimental program

Eight system configurations were tested in this study, resulting from two types of ACP, two types of insulation foam and two cavity widths. Two trials were conducted for all the combinations, for a total of 16 experiments. A nominal HRR per unit length of burner of 35 kW/m was sought, minimal variations were observed and are reported in Table 2 along with the experimental configurations tested. Each façade system was exposed to the heat from the gas burner for a different duration. Since this study is focused on the fire growth and flame spread behaviour for the façade assemblies, the burner was turned off once the measured total HRR had started to decline after reaching its peak value and had returned to initial HRR value estimated for the burner. Data logging was stopped when the measured HRR was negligible (HRR<10 kW).

The intent of this experimental program was to explore the effect of the variation of the cavity width, as well as the material properties and their interactions with other materials, on the flame spread velocity and burning rate of different cladding assemblies.

2.4. Flame height, pyrolysis height and flame spread velocity determination

All the tests were recorded on video in order to extract the flame height. The location of the flame height, identified as the tip of the continuous flame from an individual frame every 15 s was determined by analysing the recordings of the tests and correlating the location to a reference frame. The reference frame was also used to correct for visual effects because of perspective. After the location of the flame front was obtained, the spread velocity was calculated by computing the first derivative of the pyrolysis front using a second order finite difference scheme.

Additionally, a set of 20 in depth type K thermocouples (1.5 mm diameter) were installed in the insulation foam, positioned as depicted in Fig. 2 to measure the in-depth temperature distribution within the foam. Times were registered when the thermocouple readings indicated thermal decomposition was taking place in order to track the evolution of the pyrolysis front in the surface of the foam (readings for thermocouples 1 A, 2 A, 3 A, 4 A and 5 A were used for this purpose). The thermocouples recorded the advance of the pyrolysis front, indicating that the insulation foam underwent thermal decomposition when the temperature at each location reached the pyrolysis threshold.

2.5. Solid phase temperature and contribution of the system components to the fire growth

The solid phase temperatures described in the previous section were also used to estimate the HRR of the foam using the methodology proposed by Hidalgo et al. [43]. The simplified pyrolysis rate assessment consists of a two-step decoupled analysis, which first solves the heat transfer problem and then allows an estimation of the remaining mass as well as the pyrolysis rates via thermogravimetric analysis (TGA) of the materials. A sample of thickness L is divided into N finite differences of thickness (Δx_i), with i being each of the finite differences. Then, the normalised sample mass for the time step j ($\bar{m}^j$) is obtained as an integration over the space domain as per Eq. (6).

$$\bar{m}^j = \frac{\sum_{i=1}^{N}\left(\bar{m}_i^j \Delta x_i\right)}{L} \tag{6}$$

where $\bar{m}_i^j$ is the normalised mass of the finite difference (i) at the time step j which is obtained as a function of the temperature of the finite difference, $f(T)$. This function is defined by direct reference to the Thermogravimetric Analysis (TGA) for each insulation foam material. This characterisation was performed at the bench scale. Then, the normalised mass loss rate ($\dot{m}''$) can be obtained by deriving the mass loss over time, which in a discretised form corresponds to the increment of the normalised mass between time steps divided by the time step. The mass loss rate per unit area can then be calculated by considering the density of the virgin material ρ_0 and the thickness of the sample (see Eq. (7)).

$$\dot{m}'' = \rho_0 L \frac{\bar{m}^j - \bar{m}^{j-1}}{\Delta t} \tag{7}$$

Finally, the HRR for the insulation foam was calculated as the product of the effective heat of combustion ($\Delta H_{c,eff}$), the normalised mass loss rate and the area of the material (A) being burnt, using Eq. (8).

$$\dot{Q}_{INS} = \dot{m}'' \Delta H_{c,eff} A_{INS} \tag{8}$$

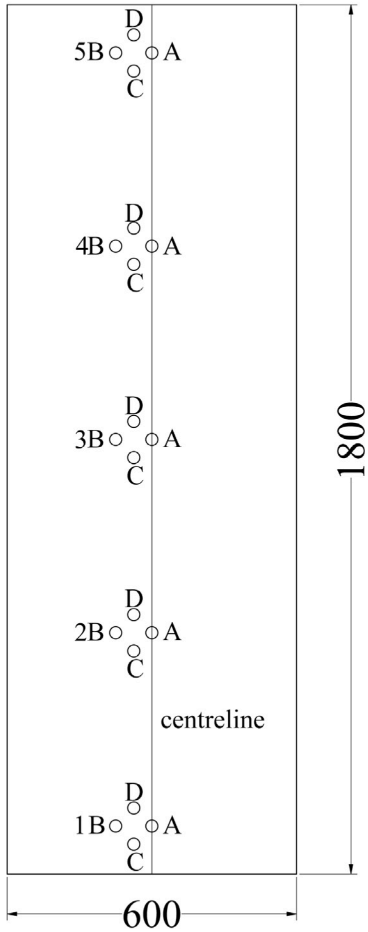

TC Code Name	Elevation (mm)	Depth (mm)	Distance from centreline (mm)
1A	100	0	0
1B	100	20	75
1C	62.5	40	37.5
1D	137.5	60	37.5
2A	500	0	0
2B	500	20	75
2C	462.5	40	37.5
2D	537.5	60	37.5
3A	900	0	0
3B	900	20	75
3C	862.5	40	37.5
3D	937.5	60	37.5
4A	1300	0	0
4B	1300	20	75
4C	1262.5	40	37.5
4D	1337.5	60	37.5
5A	1700	0	0
5B	1700	20	75
5C	1662.5	40	37.5
5D	1737.5	60	37.5

Fig. 2. In depth thermocouple location.

In this research, there was uncertainty associated with the area of the insulation being involved in the fire. It was assumed that the length of the pyrolysis area included the five 360 mm regions corresponding to the thermocouple groups (see Fig. 2). As for the width from the insulation board involved in the fire, this investigation considered minimum and maximum burning width that aligned with the experimental observations and guaranteeing that the $\dot{Q}_{INS}$ did not exceed the total HRR. The HRR of the ACPs ($\dot{Q}_{ACP}$) was then calculated as the subtraction of the HRR of the burner and the HRR of the insulation from the total HRR (determined by Oxygen Consumption calorimetry), using Eq. (9).

$$\dot{Q}_{ACP} = \dot{Q} - \dot{Q}_{INS} - \dot{Q}_{burner} \tag{9}$$

3. Results and discussion

3.1. Façade systems performance

The transient behaviour of the fire growth within the cladding assemblies is shown in Fig. 3. The fire generally spread first through the insulation foams after the foil encapsulation melted, cracked, tore or split, resulting in direct exposure of the foam; or where micro channels sustaining combustion were formed in the foam. The faster ignition of these products can be attributed to both their lower thermal inertia when compared to the ACPs and to the fact that the encapsulation of the insulation foams was thinner.

Flame spread to the top of the setup was observed for all the systems that:

(a) Featured the narrower cavity width (100 mm), regardless of the combustibility of the components. This suggests that reducing the cavity width is one factor that may promote the fire spread.
(b) Were composed of ACP PE, with a high heat of combustion, low critical heat flux for ignition of the cladding core, combined with an opposite wall reducing heat losses aiding to maintain a self-sustained combustion.

A faster flame spread rate and burnout of the system can be observed for the assemblies with ACP PE. ACP PE ignited much faster than ACP FR and presented rapid fire growth likely due to a thermal runaway process supported by the combustion of the polymeric core and the heat feedback from the flame and the opposite combustible wall. The detailed fire growth was studied through the HRR and flame height tracking and those are discussed in Sections 3.2 and 3.3 respectively.

The state of the façade materials after the tests concluded is shown in Fig. 4. It is possible to observe that for a cavity width of 0.15 m and ACP FR the flame spread was limited to a certain region of the insulation foam whereas it spread all around the insulation foam when the ACP PE was used in the system. This difference in the behaviour of the systems featuring an ACP with a combustible opposing insulation shows the impact of this material on the fire growth, not only in this combustible lining, but on the material covering the opposite wall. In this configuration the combustion of PE is self-sustaining and delivers heat to the opposite wall resulting in the combustion of the insulation which further enhances the thermal feedback in the cavity. Conversely, char formation was observed in the foam in some of the 0.15 m cavity configurations comprised of FR core.

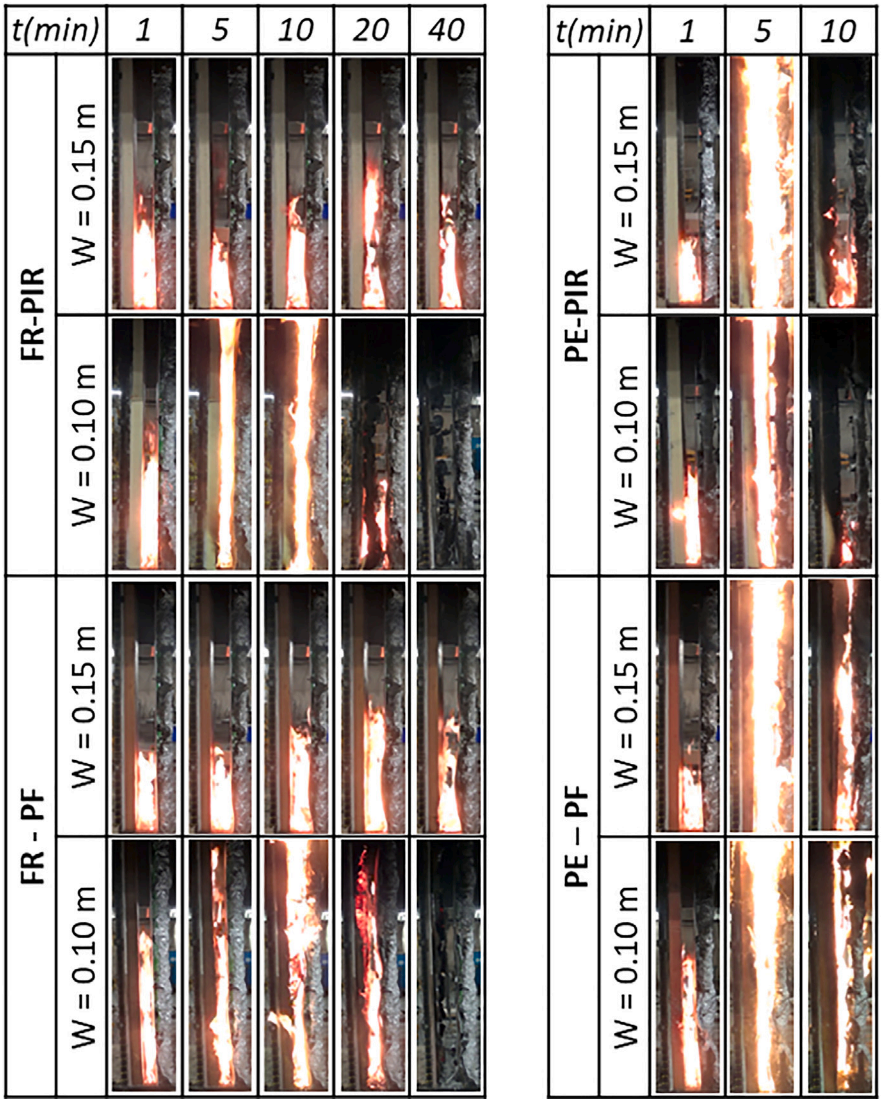

Fig. 3. Experimental behaviour of the fire growth.

This char could have acted as an insulative layer by reducing the availability of volatile combustible vapours and reducing the heat transfer of the virgin material to a value below the critical heat flux for ignition. As for the systems featuring a 0.10 m cavity it is possible to observe that more destructive results were observed for both the insulation foams and ACPs when compared to the systems featuring a wider cavity. It has been previously shown that a narrower cavity enhances the radiative thermal feedback between parallel walls [20].

The post test behaviour of the FR.PIR and FR.PF systems presented in Fig. 4 is similar to the one observed by Agarwal et al. [21] in a similar parallel panel experimental setup. Despite the experimental rig being much larger (4.9 m *x* 1.1 m vs 1.8 m *x* 0.6 m), the external heat fluxes were in a similar range to the ones in this study. An exposure of 40 kW m^{-2} was insufficient to melt the ACP encapsulation and expose the combustible cladding core, thus limiting the flame propagation to just 0.91 m above the burner. This is similar to the limited fire spread of the encapsulation in the FR.PF.150 assembly and the lack of melting of encapsulation of the ACP in the FR.PIR.150 system. Also, for a higher incident heat flux of 110 kW m^{-2}, Agarwal et al. [21] also observed the burning of the complete encapsulation and cladding core within 4 min from the start of the test. This is similar to both assemblies with a 100 mm cavity and FR ACP.

This difference in behaviour between systems with the same materials but different cavity widths is linked to the increase of the incident heat flux, which is caused by the reduction of the cavity as discussed by Mendez et al. [41].

3.2. Fire growth

The fire growth in the cladding assemblies was characterised via the total HRR. The HRR for the different façade assemblies are shown in Fig. 5.

It can be observed that for all the systems a decrease in the cavity width results in an increase on the HRR. Additionally, the time required for the encapsulation melting or cracking (and the subsequent fire growth) was reduced with a narrower cavity width. The flame did not spread beyond the area initially impinged the burner flame on the ACP installed in assemblies with a 0.15 m cavity and an FR core.

The spread over the insulation foams was limited except for the PIR-FR-R1 test, where smouldering combustion of the foam occurred and then transitioned into flaming combustion which led to flame spread to the top of the setup. This is studied in depth in the analysis of the pyrolysis front evolution (see Section 3.3). For the systems featuring ACP-FR and either insulation product the peak HRR was higher for the 0.1 m cavity than for the 0.15 m cavity. This can be attributed both to a larger amount of heat being released by the PE and a larger portion of the insulation being involved in combustion.

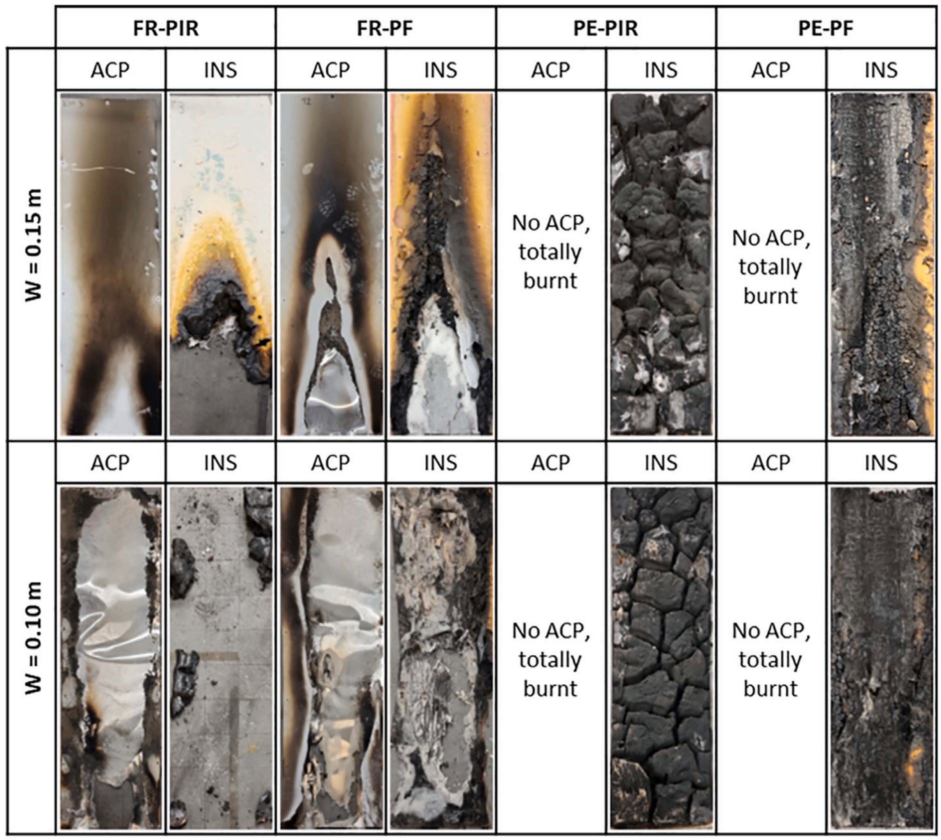

Fig. 4. Materials comprising the façade assemblies after the completion of the tests. One trial is presented per system combination.

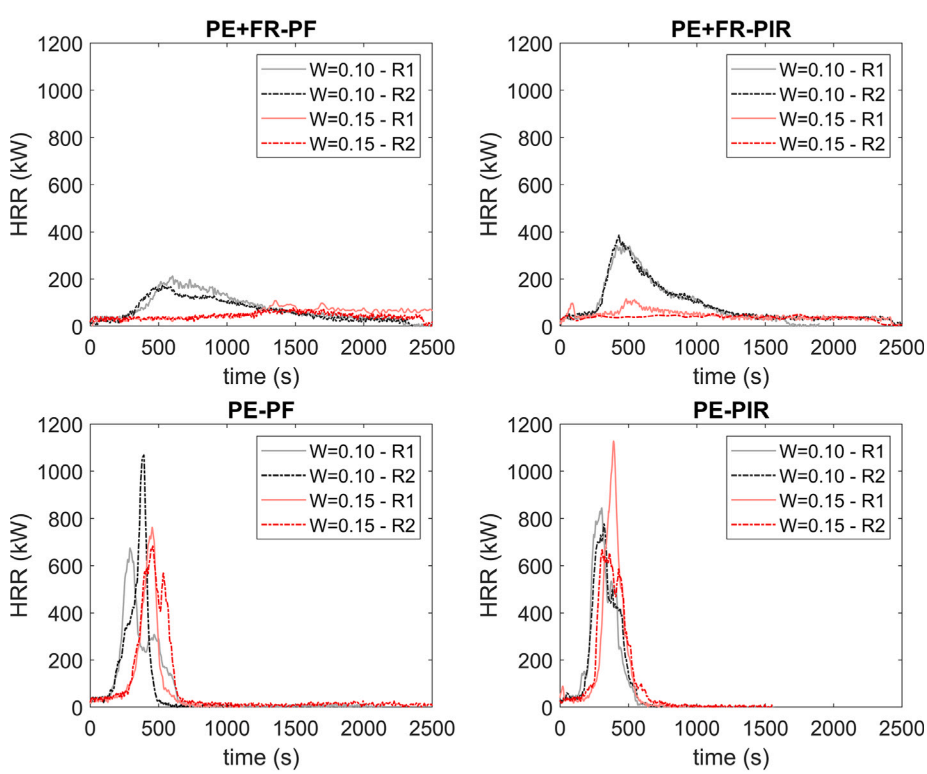

Fig. 5. Total HRR for the different façade assemblies.

Two fire growth "stages" were observed for the assemblies with a FR ACP, the first consisting of the flame spread over the insulation encapsulation and the insulation itself, and a subsequent flame spread over ACP once the ACP encapsulation melted or detached from the organic core. These two phenomena were previously observed in a number of full-scale tests commissioned by the UK Government, where the interactions between different ACPs and insulations separated by a cavity were observed [44]. Melting of the ACP encapsulation was generally followed by the increase of the HRR once the polymeric ACP core was thermally degraded. The ACP breach generally agrees with the increase of the HRR. This is further explored in Section 3.4 where the different stages are presented by quantifying the HRR of the ACPs and insulation foams separately. Also, for these cladding assemblies, a faster increase of the HRR can be observed for the assemblies comprised of PIR compared to the ones comprised of PF, this is consistent with the behaviour presented at bench scale for the HRR of the insulation cores [45], since a higher HRR of the combustible material generates a faster flame spread.

The influence of the cavity on the fire growth rate highlights the importance of considering the interactions of the material with the system in which it will be installed and how those interactions could affect its performance.

3.3. Flame length, pyrolysis length and fire growth

Flame length can be used as an indicator for fire growth. Fig. 6 presents the flame heights for the façade assemblies. The dotted dashed black line represents the height of the setup, measurements beyond that height are presented for illustrative purposes only, since they surpass the parallel wall configuration studied in this research therefore are unconstrained flames outside of the cavity.

The flame height profiles are consistent with the behaviour presented in the HRR profiles. Flame height increase is observed earlier for a narrower cavity width for all the cladding assembly configurations. This behaviour can be linked to the increase in the thermal feedback with the space between the walls being reduced, as observed by Mendez et al. [41]. Additionally, the flame length increases faster and this increase happens more rapidly in the assemblies comprised of PE when compared with the ones featuring FR cores. This faster flame height increase can be linked to a higher HRR in said systems, observed both in medium scale (see Fig. 5) and bench scale characterisation [3]. Also, a faster flame length increase was observed for the assemblies comprised of FR-PIR versus the ones comprised of FR-PF, which agrees with the behaviour observed at bench scale.

Focus was made on the fire growth stage since it was observed that the HRR decay was mainly explained by the consumption of the cladding materials, making this phenomenon heavily influenced by the setup. Hence, the flame height and pyrolysis front for the fire growth stage were extracted and are presented in Fig. 7 for all the experiments. The fire growth stage was defined as the data up to the time when L_p length presented an increase; or before L_p reached 1.7 m, corresponding to the maximum measurable distance given the TC locations. Faster pyrolysis front advancement can be observed for the assemblies with a narrower cavity. This is evident as the data series of pyrolysis length versus time for the narrower cavity width (0.10 m, circles) present a steeper increase than the ones for the wider cavity (0.15 m, squares). This can be associated with the aforementioned enhanced thermal feedback between the two walls, which provides a larger incident heat flux, thus decreasing the time required for ignition, and increasing the flame spread velocity (see Eq. (2)). This faster pyrolysis translates into a more rapid combustion, exhibited in both the assemblies comprised of PE, regardless of the cavity width and for all the systems with the narrower cavity. The pyrolysis length was then used to parameterise and quantify the fire growth rate as proposed by Orloff et al. [10].

Table 3
Fire growth rate.

System	γ (1/s)	R^2
FR-PF-W150	0.002 ± 0.001	0.878
FR-PIR-W150	0.005 ± 0.001	0.799
PE-PF-W150	0.005 ± 0.001	0.969
PE-PIR-W150	0.018 ± 0.006	0.266
FR-PF-W100	0.010 ± 0.003	0.492
FR-PIR-W100	0.009 ± 0.001	0.758
PE-PF-W100	0.012 ± 0.001	0.893
PE-PIR-W100	0.011 ± 0.002	0.921

Eq. (4) was used in order to determine the fire growth rate (γ). A growth rate was determined for each cladding assembly configuration and the results for this factor are presented in Table 3.

The proposed models based on the fire growth parameter (γ)) are presented in Fig. 8. The experimental fit adjusts properly for most of the configurations, except for the PE-PIR-W150 and FR-PF-W100 systems.

In general, systems with a narrower cavity width showed a larger growth factor, i.e., faster flame spread. It should be noted that this model was initially developed for upward flame spread on a single slab of PMMA (45 mm thick, 410 mm wide, 1570 mm high), with experimental values for γ ranging between 0.0037 and 0.0039 s^{-1} [10]. These results similar to the values obtained for the systems with a wider cavity width (W150) and FR ACPs. The comparison cannot be made in a straightforward manner since the materials (PMMA vs other encapsulated materials), their dimensions and the system geometry (single wall vs parallel wall) differ between the two studies, but it is reasonable to expect that the encapsulation will delay the fire growth, resulting in a lower growth factor, observed in the parallel wall configuration.

Conversely, for systems with ACP PE and the narrower cavity width (W100) the values for gamma were much higher. Both the heat released by the PE core and the higher thermal feedback with a closer opposite wall create a higher incident flux on the opposite wall, hence accelerating the flame spread.

The cavity width has a significant effect on the fire growth for the systems comprised of an FR core with the growth factor being twice larger, and also reaching similar growth rate parameters to the systems comprised of PE when the cavity is reduced from 0.15 to 0.10 m. In this case the narrower cavity enhanced the heat transfer to the encapsulation and core, leading to the combustion of a larger area of the ACP, hence to a larger HRR, flame height and to a faster fire growth [41]. Conversely, there is no evident effect of the cavity width when comparing the assemblies comprised of PE and any of the insulations. In this, case the ACP walls were consumed faster when a narrower cavity was used, hence eliminating the second wall and reducing the thermal feedback between the surfaces. The energy that was initially kept inside the cavity was now transferred to the surroundings, thus decelerating the combustion of the insulation foam. These contributions were also studied through the quantification of the HRR of each of the components of the façade.

3.4. Component contribution to HRR

The use of a high density of instrumentation enabled the use of bench scale flammability data for the interpretation and micro-scale data (TGA analysis) for the decoupling of the contribution of the materials to the total HRR. The contribution of the cladding materials was further explored by quantifying the heat released by each material. Fig. 9 presents a subset of the results for the HRR for each of the components of a cladding assembly comprised of PF and FR. For both systems an initial stage is observed, in which the insulation binding agent and the adjacent polymeric core burns. For the wider cavity (W = 0.15 m), a portion of the PF insulation (INS) was involved in a limited amount of fire growth i.e., unsustained. This decayed once a char layer was formed and the flame failed to establish on the ACP

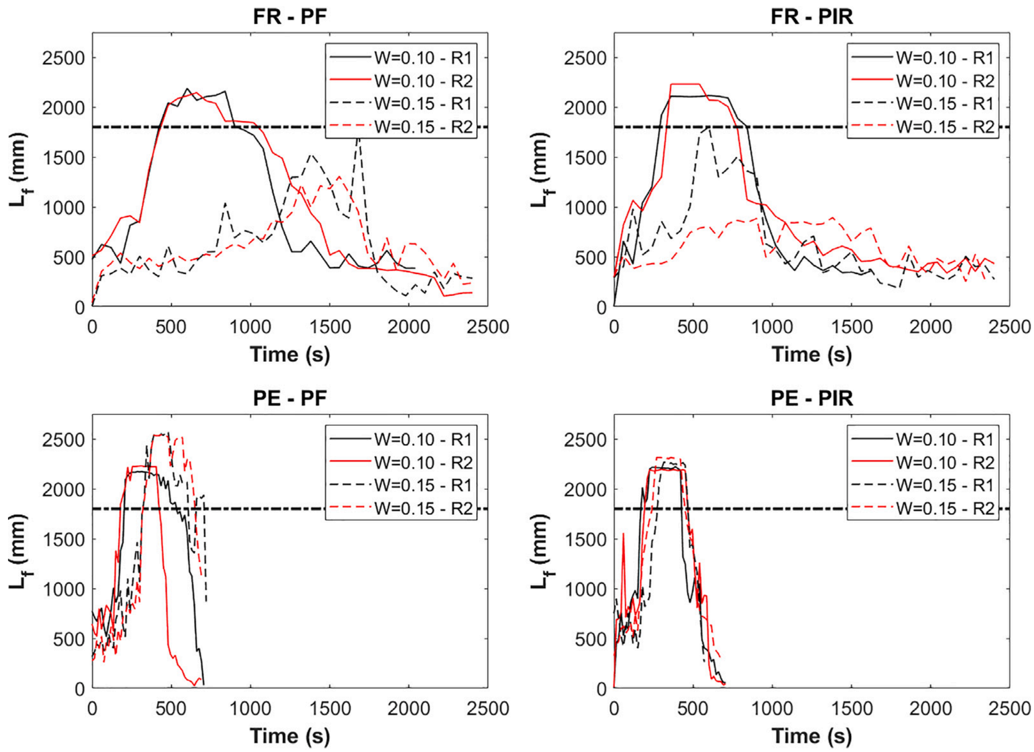

Fig. 6. Transient flame heights.

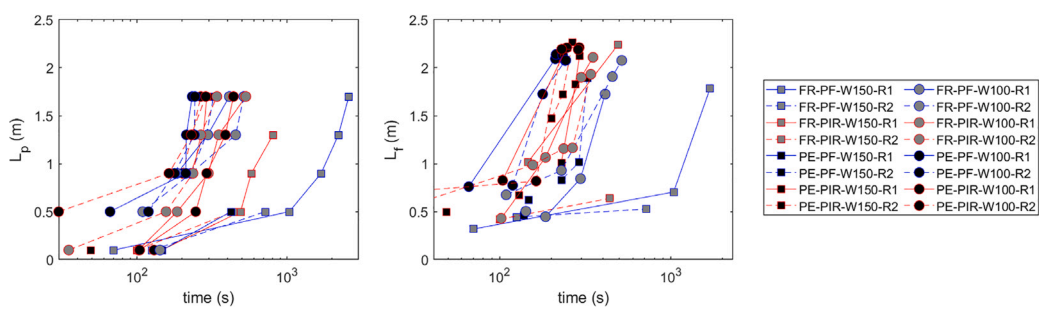

Fig. 7. Pyrolysis front and flame height evolution. The time is presented in a logarithmic scale to help the visualisation of the data.

core. A final period of fire growth was observed due to remaining smouldering combustion that transitioned into flaming combustion at t ≈ 2000 s.

For the narrower cavity, the initial fire growth progressed in a similar manner, with initial burning of the PF. The additional HRR from the burning PF and the thermal feedback between the walls of the cavity led to two further stages of fire growth: the melting of the aluminium encapsulation and subsequent rapid fire growth once the polymeric ACP core was thermally degraded. It can be observed that the FR core provided a greater contribution to the overall HRR for the rest of the experiment. This comparison shows the effect of the cavity on the interaction of components and its potential for the development of different fire scenarios involving the same cladding components. A similar trend was observed for the rest of the configurations. Hence, it shows how materials that could be initially deemed to perform in one way could perform in a different way when interacting with other design elements, e.g., a narrower cavity.

The contribution of the cladding materials to the total HRR for the cladding assemblies featuring PIR is presented in Fig. 10, all the combinations of ACPs and cavity widths are shown.

The combustible insulation materials (PIR and PF) contributed to the HRR and fire growth earlier than the ACP cores for all of the configurations with the contribution of PIR being larger than for PF, which is consistent with the HRR data at the bench scale. The insulation type had no significant effect on the fire growth on assemblies using PE, since this material dominated the combustion process. It can be observed that a narrower cavity width resulted in a larger contribution from the PIR foam when FR was used in the ACP core (Fig. 10(a) and (b)).

A higher thermal feedback generated a greater incident heat flux over a larger area of the insulation leading to a larger HRR of this cladding material, thus enhancing the fire growth and sustaining flaming combustion over the ACP. A different phenomenon is observed for the systems comprised of a PE core (Fig. 10(c) and (d)), since a faster consumption of the ACP and its encapsulation layers was observed. The absence of a second wall due to the rapid burning of the ACP panel, reduced the thermal feedback generating a lower involvement of the insulation on the overall HRR. Additionally, drastic differences in the performance of systems using PE versus FR were observed. Those differences were expected considering the differences in the flammability properties of these two cores, previously observed at the smaller scale by McLaggan et al. [42], at bench scale. A large contribution from the ACP core can be observed at an early stage of the HRR in Fig. 10(c).

A large contribution from the ACP core to the total HRR is contradictory to the experimentally observed behaviour and can be attributed

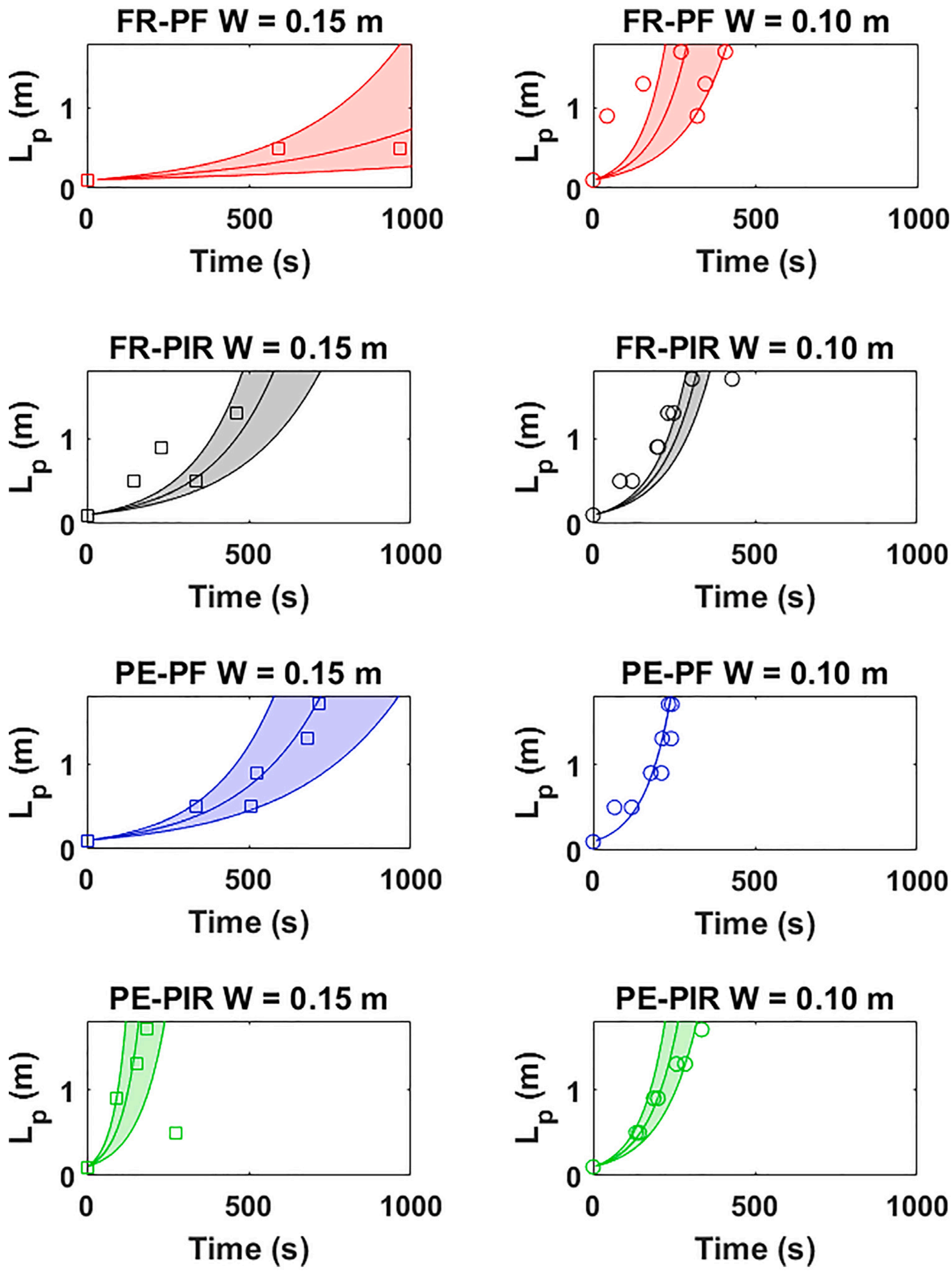

Fig. 8. Proposed fire growth model vs experimental data. The markers represent the experimental data and the shaded area includes the minimum and maximum pyrolysis lengths with the values estimated for γ.

to the combustion of the binding agent of the PIR and how the contribution of the ACP to the total HRR is calculated by the subtraction of the burner HRR and the INS HRR from the total HRR, i.e., the contribution of any materials besides the polymeric cores was neglected (see Eq. (9)). The influence of insulation foam on a specific ACP material cannot be easily anticipated at this stage and the results of this research are limited to the materials comprising the studied systems being exposed to a fire spreading on the inner side of a cavity. The findings of this study emphasise the need to gain a comprehensive understanding of the interactions between insulation materials and ACPs. Extrapolation of these results to larger scales should be made carefully since, in real scale the ACP might be exposed to fire from both the inner and external sides of the cavity which might affect the flame spread behaviour. Further research is necessary to analyse these interactions in order to enhance the ability to evaluate the fire performance of cladding systems more accurately.

3.5. Simplified theoretical framework for flame spread in a ventilated façade

Fig. 11 presents a framework simplified framework for flame spread in a ventilated façade based on the fire behaviour of the 8 systems tested in this study. The fire growth occurred after the insulation encapsulation breached for all of the tested configurations (i.e., the system configuration generated a lining heat exposure high enough to breach the aluminium foil encapsulation in the initial stages of the experiments). The effect of the cavity width is highlighted, considering that a narrower cavity width enhances the heat transfer to the linings, as observed by Mendez et al. [20]. Then, two positive fire growth feedback loops are shown linking the heat released by the combustible products to the incident heat flux necessary to sustain the combustion and flame spread. The positive feedback loops involve self-reinforcing

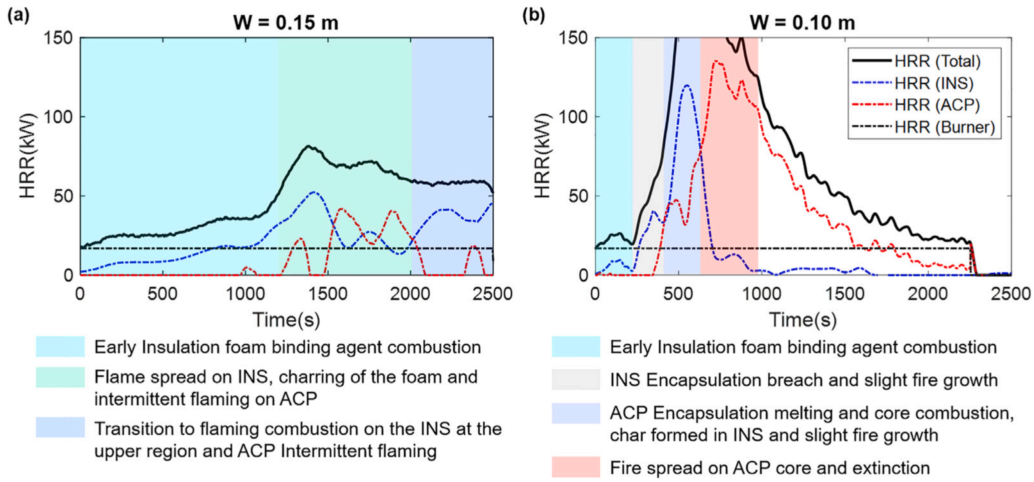

Fig. 9. HRR contributions for (a) PF-FR-W150 and (b) PF-FR-W100 façade systems.

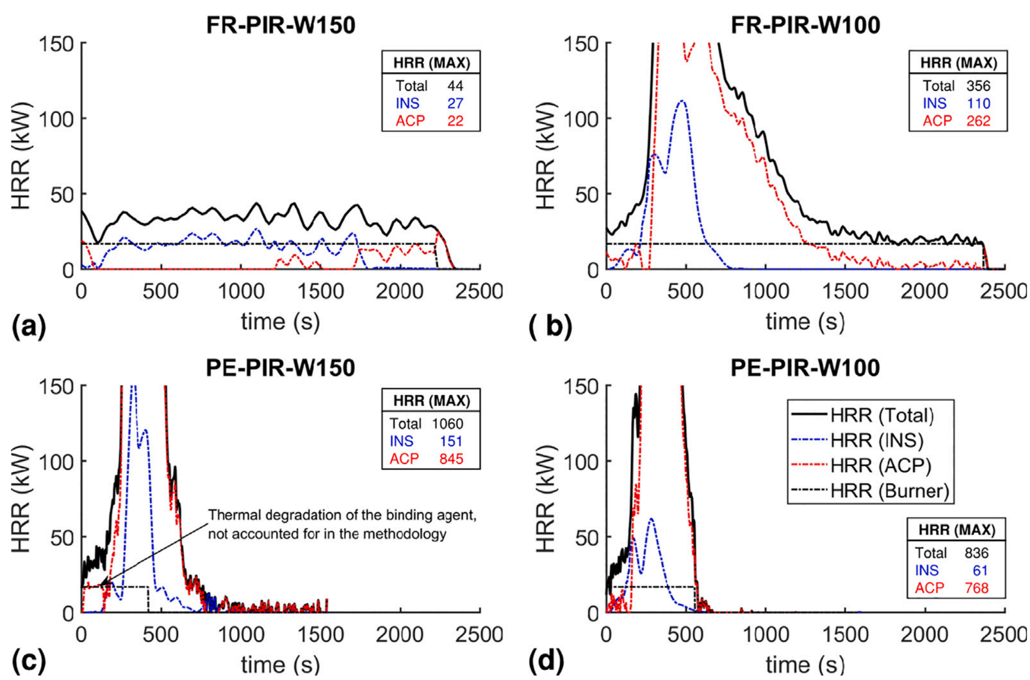

Fig. 10. HRR contributions for (a) PIR-PE-W150, (b) PIR-PE-W100, (c) PIR-FR-W150, (d) PIR-FR-W100 façade systems. The scale of the HRR has been limited to compare the contribution of the materials.

mechanisms that promote the continuous supply of heat (incident heat flux) and fuel (increase of HRR), sustaining the fire. These loops enhance the combustion process and facilitate the release of flammable gases, further feeding the flames. These positive feedback loops are the manifestation at a larger scale of phenomena identified at smaller scales [3]. The critical element for the fire growth is the incident heat flux received by the material.

In the case of the insulation foam the threshold value was associated to the critical heat flux of ignition of the foam itself ($\dot{q}''_{cr,ig}$ (INS)), since the encapsulation of this material was breached easily, almost after the burner ignition. The threshold value of heat flux required for melting the ACP core ($\dot{q}''_{melt}$ (ACP,encaps)) was chosen, since fire growth was observed to accelerate after the melting of the aluminium encapsulation.

In contrast, the negative feedback loops act as self-regulating mechanisms that hinder fire progression. They involve processes such as depletion of available fuel sources and the consolidation of a thick char layer. These loops counteract the fire's development, leading to a reduction in heat release and eventual extinguishment.

By illustrating the interconnected feedback loops, the diagram highlights the complex dynamics and potential outcomes of a fire scenario. The framework also highlights those material and system parameters that are needed in order to be able to determine the behaviour of façade assemblies comprising different geometries and fuels.

4. Conclusions

This study presents a methodology for assessing the contribution of cavity width and material properties to fire growth in ventilated façade systems. Eight configurations were tested using two ACPs (PE and FR), two insulation foams (PIR and PF), and two cavity widths (0.10 m and 0.15 m). The interactions between these materials and their impact on fire dynamics were characterised, providing insight into the flammability behaviour and thermal feedback mechanisms that govern upward flame spread.

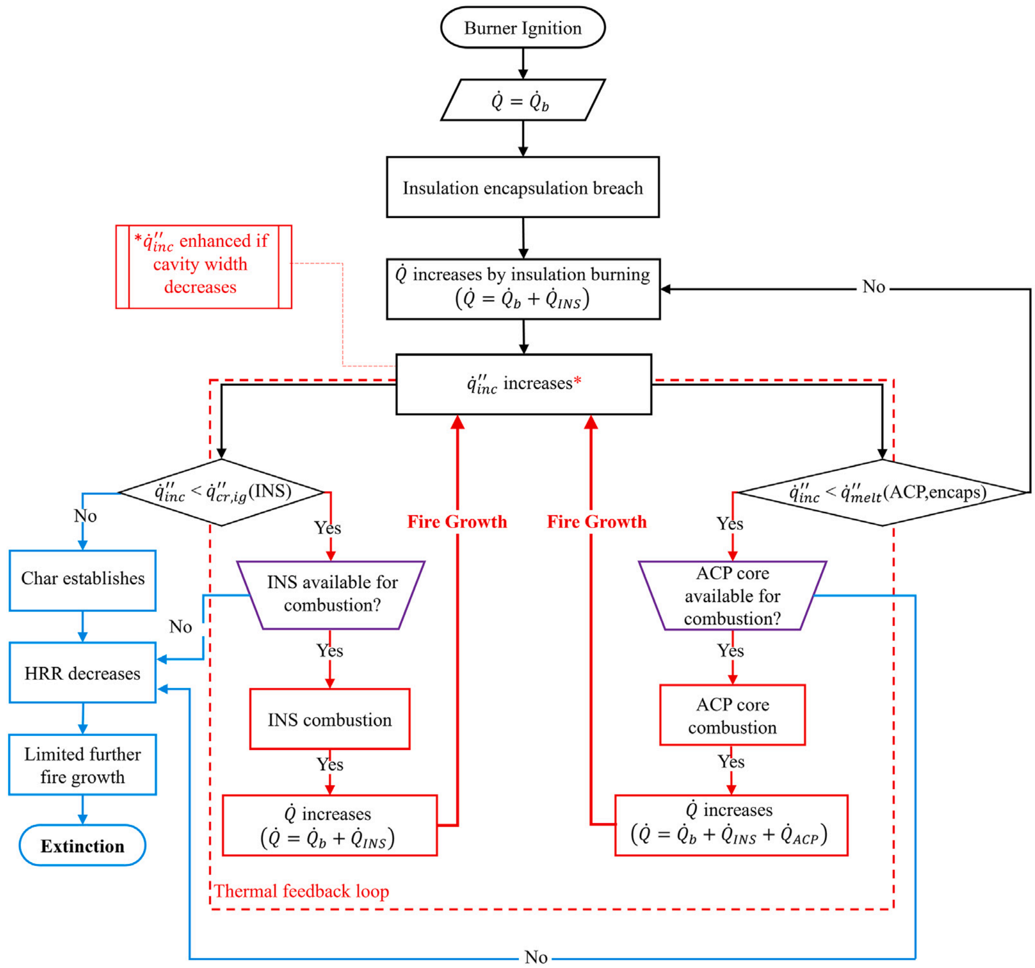

Fig. 11. Theoretical framework for flame spread in a ventilated façade.

The medium-scale experimental approach proved effective in analysing material interactions and fire propagation in ventilated façades. The high-density instrumentation allowed the use of bench-scale flammability data and micro-scale thermal analysis (TGA) to interpret material contributions to total HRR. While direct extrapolation from smaller to medium scales remains challenging, the results indicate the potential for a comprehensive framework to assess fire performance across different material combinations and system layouts. Such a framework could enhance the design and evaluation of fire-safe building exteriors, supporting improved fire safety regulations.

Observations from this study align qualitatively with large-scale façade fire tests conducted in the UK [44]. However, further research is needed to quantitatively connect material-scale models and heat transfer mechanisms to full-scale fire behaviour. One critical finding was that the loss of encapsulation integrity triggered fire growth and accelerated flame spread over combustible linings. Although encapsulation failure was beyond this study's scope, its influence on façade fire behaviour warrants further investigation.

Reducing the cavity width was found to enhance thermal feedback, accelerating encapsulation failure and polymer degradation. Insulation materials (PIR and PF) contributed to fire growth early, with PIR exhibiting higher HRR values than PF, consistent with bench-scale data. Smoldering combustion was more pronounced in PF but was also observed in PIR, potentially sustaining or reactivating flaming combustion.

The insulation type had limited impact on ACP-PE assemblies, where the PE core dominated fire behaviour. However, for larger cavity widths, PIR exhibited faster fire growth than PF, influencing peak HRR values, particularly in FR configurations. This suggests that material interactions and cavity geometry play a critical role in overall façade fire performance.

While material classification alone does not fully quantify fire spread within a system, the Cladding Materials Library framework provided a reliable interpretation of the governing fire dynamics. A theoretical framework was developed to describe key interactions between material properties, system variables, and fire spread mechanisms. The study identified positive feedback loops in fire propagation and key material properties – such as char formation and heat release limitations – that influence the ability of façade components to either sustain or inhibit flame spread.

CRediT authorship contribution statement

Julian E. Mendez: Writing – original draft, Visualization, Investigation. **Martyn S. McLaggan:** Writing – review & editing, Supervision, Conceptualization. **David Lange:** Writing – review & editing, Supervision, Conceptualization.

Declaration of competing interest

The authors declare that they have no known competing financial interests or personal relationships that could have appeared to influence the work reported in this paper.

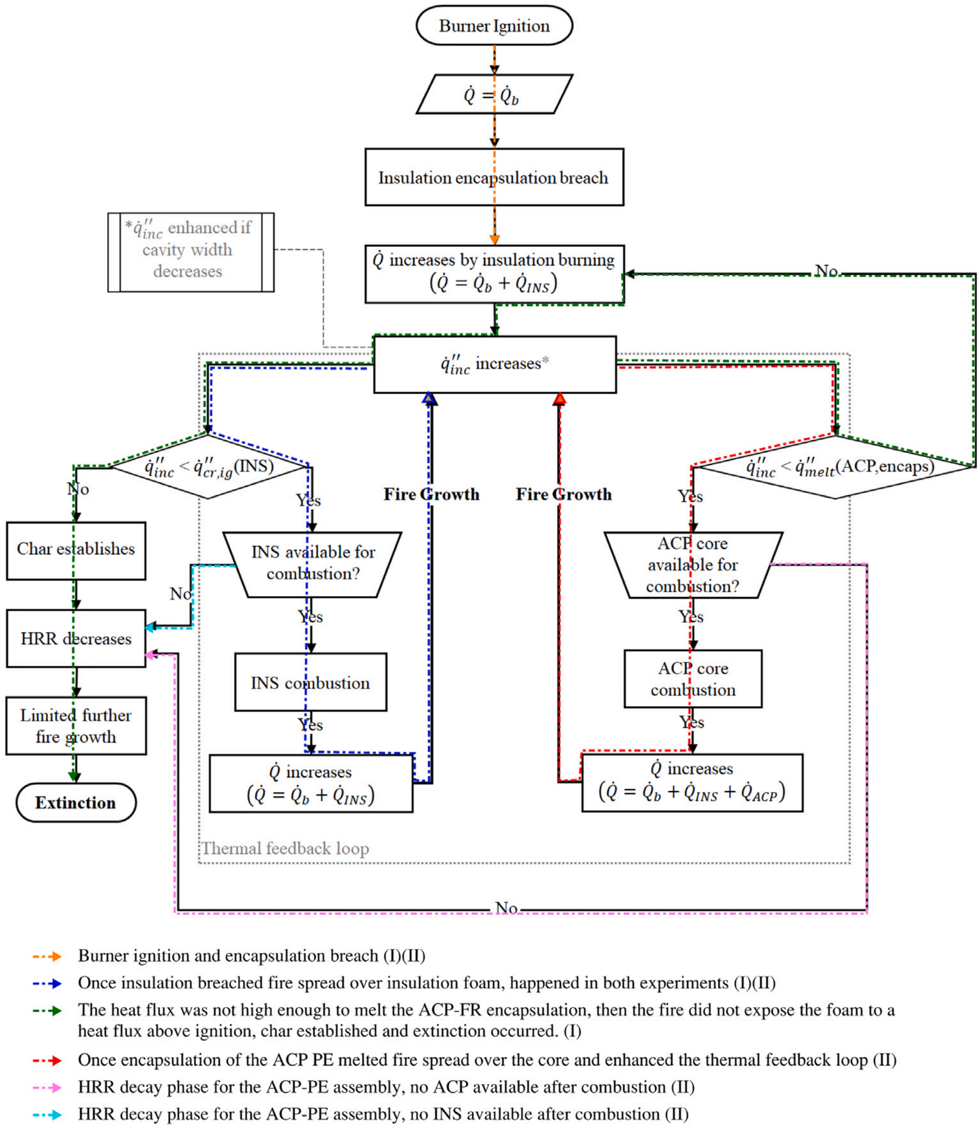

Fig. 12. Application of the theoretical framework to two different assemblies:(I): FR.PIR.W150 and (II): PE.PIR.W150. The events summarising the behaviour of the assemblies have been added as coloured lines.

Appendix

A.1. Application of the simplified theoretical framework for flame spread in a ventilated façade

Fig. 12 shows the use of the proposed framework to describe the behaviour of two different assemblies :

- FR.PIR.W150 **(I)**, which comprised ACP-FR and did not lead to flame spread on the cladding core; and
- PE.PIR.W150 **(II)**, which comprised ACP-PE which lead to flame spread both on the insulation foam and on the cladding core.

It can be seen from Fig. 12 that a system comprising cladding with FR core and a larger cavity (I) width only presented limited flame spread on the insulation foam, just in the region where the heat flux generated by the configuration exceeded the critical heat flux for ignition. The regions of the foam located further away were protected by the char formed on the surface or did not receive enough heat to cause ignition. Conversely, for the façade system featuring a PE core in the cladding, the initial combustion of the PIR foam lead to the ACP encapsulation melting, which subsequently generated the combustion of the ACP core and increased the incident heat flux on both linings. The HRR of the system just decreased as a result of the combustion of the entirety of the insulation and cladding panels.

Data availability

Data will be made available on request.

References

[1] J.L. Torero, Grenfell tower inquiry - phase 2 - adequacy of the current testing regime (JTOR00000006), 2022, pp. 1–240.
[2] M.S. McLaggan, V. Gupta, J.P. Hidalgo, J.L. Torero, Upward flame spread for fire risk classification of high-rise buildings, Int. J. High- Rise Build. 10 (4) (2021) 299–310, http://dx.doi.org/10.21022/IJHRB.2021.10.4.299.
[3] J. Mendez, Characterisation of the fire dynamics in ventilated façades (PhD thesis), 2024, http://dx.doi.org/10.14264/bad326e.
[4] F.A. Williams, Mechanisms of fire spread, Symp. (International) Combust. 16 (1) (1977) 1281–1294, http://dx.doi.org/10.1016/S0082-0784(77)80415-3.
[5] J.G. Quintiere, A theoretical basis for flammability properties, Fire Mater. 30 (3) (2006) 175–214, http://dx.doi.org/10.1002/FAM.905.

[6] H.S. Carslaw, J.C. Jaeger, Conduction of heat in solids, second ed., Clarendon Press, 1959.
[7] R.F. McAlevy, R.S. Magee, The mechanism of flame spreading over the surface of igniting condensed-phase materials, Symposium (International) on Combustion 12 (1) (1969) 215–227, http://dx.doi.org/10.1016/S0082-0784(69)80405-4.
[8] A.C. Fernandez-Pello, Downward flame spread under the influence of externally applied thermal radiation, Combust. Sci. Technol. 17 (1–2) (1977) 1–9, http://dx.doi.org/10.1080/00102209708946807.
[9] A.C. Fernandez-Pello, Upward laminar flame spread under the influence of externally applied thermal radiation, Combust. Sci. Technol. 17 (3–4) (1977) 87–98, http://dx.doi.org/10.1080/00102207708946818.
[10] L. Orloff, J. De Ris, G.H. Markstein, Upward turbulent fire spread and burning of fuel surface, Symp. (International) Combust. 15 (1) (1975) 183–192, http://dx.doi.org/10.1016/S0082-0784(75)80296-7.
[11] A.C. Fernandez-Pello, A theoretical model for the upward laminar spread of flames over vertical fuel surfaces, Combust. Flame 31 (C) (1978) 135–148, http://dx.doi.org/10.1016/0010-2180(78)90124-4.
[12] B. Karlsson, Models for calculating flame spread on wall lining materials and the resulting heat release rate in a room, Fire Saf. J. 23 (4) (1994) 365–386, http://dx.doi.org/10.1016/0379-7112(94)90004-3.
[13] G.H. Markstein, J. de Ris, Upward fire spread over textiles, Symp. (International) Combust. 14 (1) (1973) 1085–1097, http://dx.doi.org/10.1016/S0082-0784(73)80098-0.
[14] M. Sibulkin, J. Kim, The dependence of flame propagation on surface heat transfer II. Upward burning, 17 (1977), 1977, pp. 39–49, http://dx.doi.org/10.1080/00102209708946811.
[15] J. Quintiere, M. Harkerload, Y. Hasemi, Wall flames and implications for upward flame spread, Combust. Sci. Technol. 48 (1986) 191–222, http://dx.doi.org/10.1080/00102208608923893.
[16] K.C. Tsai, J. Turnbull, G. Will, D. Drysdale, Upward flame spread: Heat transfer to the unburned surface, Fire Saf. Sci. (2003) 117–128, http://dx.doi.org/10.3801/IAFSS.FSS.7-117,
[17] G. Back, C. Beyler, P. Dinenno, P. Tatem, Wall incident heat flux distributions resulting from an adjacent fire, Fire Saf. Sci. 4 (1994) 241–252, http://dx.doi.org/10.3801/iafss.fss.4-241.
[18] M. Foley, D.D. Drysdale, Heat transfer from flames between vertical parallel walls, Fire Saf. J. 24 (1995) 53–73, http://dx.doi.org/10.1016/0379-7112(94)00033-c.
[19] K. Livkiss, S. Svensson, B. Husted, P. van Hees, Flame heights and heat transfer in façade system ventilation cavities, Fire Technol. 54 (2018) 689–713, http://dx.doi.org/10.1007/s10694-018-0706-2.
[20] J. Mendez, J.P. Hidalgo, D. Lange, M.S. Mclaggan, Effect of cavity parameters on the fire dynamics of ventilated façades, Fire Saf. J. 133 (2022) 103671, http://dx.doi.org/10.1016/j.firesaf.2022.103671.
[21] G. Agarwal, Y. Wang, S. Dorofeev, Fire performance evaluation of cladding wall assemblies using the 16-ft high parallel panel test method of ANSI/FM 4880, Fire Mater. 45 (5) (2020) 609–623, http://dx.doi.org/10.1002/fam.2852.
[22] K.C. Tsai, Upward flame spread on a flat surface, in a corner and between two parallel surfaces, J. Chin. Soc. Mech. Eng. Trans. Chin. Inst. Eng. - Ser. C 28 (2007) 341–348.
[23] R. Schlyter, Av statens provningsanstalt godkanda byggnadskonstruktioner I de olika brandtekniska klass erna - testing of the fire–resistance of building materials and structures), Statens Provningsanst. Stock. Medd. Stock. Medd. 66 (1935).
[24] R. Schlyter, Eldskyddspreparat för träkonstruktioner och textilier, Technical Report, RISE, SP – Sveriges Provnings- och Forskningsinstitut, SP – Sveriges Tekniska Forskningsinstitut, RISE, 1939, 2023-03-09T09:14:38.537+01:00.
[25] L. Markwardt, H. Bruce, A. Freas, Brief Descriptions of Some Fire-Test Methods Used for Wood and Wood-Base Materials, Technical Report, USDA, United States Department Of Agriculture - Forest Service, 1954.
[26] V. Babrauskas, The grenfell tower fire and fire safety materials testing, Fire Eng. (2018).
[27] S.L. LeVan, C.A. Holmes, Effectiveness of Fire-retardant Treatments for Shingles After 10 Years of Outdoor Weathering, Technical Report, USDA, 1986.
[28] M.A. Dietenberger, C.R. Boardman, HRR upgrade to mass loss calorimeter and modified schlyter test for fr wood, in: Proceedings of the Fire and Materials 2013 Conference, Citeseer, 2013, p. 25.
[29] H.-Y. Shih, H.-C. Wu, An experimental study of upward flame spread and interactions over multiple solid fuels, J. Fire Sci. 26 (5) (2008) 435–453, http://dx.doi.org/10.1177/0734904108092547.
[30] K. Choi, W. Taylor, Combustibility of insulation in cavity walls, J. Fire Sci. 2 (3) (1984) 179–188, http://dx.doi.org/10.1177/073490418400200303.
[31] W. Taylor, Fire spread in concealed foamed plastic insulation, Fire Technol. 19 (3) (1983) 192–203, http://dx.doi.org/10.1007/BF02378699/METRICS.
[32] J. De Ris, L. Orloff, Flame heat transfer between parallel panels, Fire Saf. Sci. 8 (2005) 999–1010, http://dx.doi.org/10.3801/iafss.fss.8-999.
[33] S. Nam, Intermediate-scale fire test? Stepping stone for prediction of material flamability in real-scale fire through bench-scale fire test data, Fire Saf. Sci. 7 (2007) 27–45.
[34] L. Bisby, Grenfell Tower Inquiry: Professor Luke Bisby report (Phase 2 - Experiments Work Package 2- System Interactions), LBYWP200000001, Technical Report December, University of Edinburgh, 2021, pp. 1–130.
[35] A. Sharma, K.B. Mishra, Experimental investigations on the influence of 'chimney-effect' on fire response of rainscreen façades in high-rise buildings, J. Build. Eng. 44 (2021) 103257, http://dx.doi.org/10.1016/j.jobe.2021.103257.
[36] E. Guillaume, T. Fateh, R. Schillinger, R. Chiva, S. Ukleja, R. Weghorst, Intermediate-scale tests of ventilated facades with aluminium-composite claddings, J. Physics: Conf. Ser. 1107 (2018) 032007, http://dx.doi.org/10.1088/1742-6596/1107/3/032007.
[37] B. Garvey, J. Ogilvie, J. Carrascal, D. Lange, C. Maluk, M.S. McLaggan, A. Osorio, J.L. Torero, J.P. Hidalgo, Experimental methodology to study the fire contribution of cladding materials, in: Interflam, vol. 15, 2019, pp. 2079–2090.
[38] Department of Housing and Public Works, Non-Conforming Building Products Audit Taskforce, Queensland non-conforming building products audit taskforce - status report, 2018, URL https://www.hpw.qld.gov.au/_data/assets/pdf_file/0022/5719/claddingtaskforcereport.pdf.
[39] M. McLaggan, J. Hidalgo, A. Osorio, M. Heitzmann, J. Carrascal, D. Lange, C. Maluk, J. Torero, Towards a better understanding of fire performance assessment of façade systems: Current situation and a proposed new assessment framework, Constr. Build. Mater. 300 (2021) 124301, http://dx.doi.org/10.1016/j.conbuildmat.2021.124301.
[40] X. Sun, H. Yoshioka, T. Noguchi, Y. Nishio, B. Zhou, Experimental and numerical investigations of cavity flame spread in double skin façade, Case Stud. Therm. Eng. 65 (2025) 105607, http://dx.doi.org/10.1016/j.csite.2024.105607, URL https://www.sciencedirect.com/science/article/pii/S2214157X24016381.
[41] J.E. Mendez, M.S. McLaggan, D. Lange, Upward flame spread behaviour of cladding materials on a medium-scale ventilated façade experimental setup with a single combustible wall, Fire Saf. J. (Accept. under Revision) (2023) http://dx.doi.org/10.1016/j.firesaf.2023.104020.
[42] M.S. McLaggan, J.P. Hidalgo, M. Heitzmann, A.F. Osorio, C. Maluk, D. Lange, J. Carrascal, J.L. Torero, Protocols for the Material Library of Cladding Materials – Part II: Sample preparation and testing methodologies, Technical Report July, The University of Queensland, St Lucia, 2019, pp. 1–22, URL https://espace.library.uq.edu.au/view/UQ:1d87ca0.
[43] J.P. Hidalgo, N. Gerasimov, R.M. Hadden, J.L. Torero, S. Welch, Methodology for estimating pyrolysis rates of charring insulation materials using experimental temperature measurements, J. Build. Eng. 8 (2016) 249–259, http://dx.doi.org/10.1016/j.jobe.2016.09.007.
[44] BRE Global, BRE Global Client Report – BS8414-1:2015 A1:2017 Test, DCLG test 1, Watford, UK, 2017, Technical Report, Department for Communities and Local Government, 2017, URL https://www.gov.uk/government/uploads/system/uploads/attachment_data/file/648789/DCLGtest1_BS_8414_Part_1_test_report_Issue1.2.pdf. (Online; accessed 2023-07-19).
[45] M.S. McLaggan, J.P. Hidalgo, A.F. Osorio, M. Heitzmann, J. Carrascal, D. Lange, C. Maluk, J.L. Torero, The material library of cladding materials, data collection, 2019, http://dx.doi.org/10.14264/uql.2019.441.